IEEE Access
Multidisciplinary | Rapid Review | Open Access Journal

Received August 16, 2018, accepted September 14, 2018, date of publication September 19, 2018, date of current version October 17, 2018.

*Digital Object Identifier 10.1109/ACCESS.2018.2871068*

# Slotted ALOHA for Wireless Powered Communication Networks

**HYUN-HO CHOI[1], (Member, IEEE), AND WONJAE SHIN[2,3], (Member, IEEE)**
[1]Department of Electrical, Electronic and Control Engineering, Hankyong National University, Anseong 17579, South Korea
[2]Department of Electronics Engineering, Pusan National University, Busan 46241, South Korea
[3]Department of Electrical Engineering, Princeton University, Princeton, NJ 08540, USA

Corresponding author: Wonjae Shin (wjshin@pusan.ac.kr)

This work was supported by the Basic Science Research Program through the National Research Foundation of Korea (NRF) funded by the Ministry of Science, ICT & Future Planning under Grant NRF-2016R1C1B1016261.

**ABSTRACT** Centralized controls in wireless-powered communication networks (WPCNs) induce considerable overhead for channel estimation and high complexity for optimization, as the number of wireless devices (WDs) increases. To tackle this problem, we apply slotted ALOHA protocol to WPCNs and design a slotted ALOHA-based energy-harvesting medium access control protocol. In this protocol, the WD randomly selects one of the given random access (RA) slots and continuously harvests the energy from the hybrid access point (HAP) until it has access. We analyze the average channel throughput and obtain the optimal number of RA slots allocated ($m^*$) to maximize it. Thereafter, we present a prioritized access control to alleviate the doubly near-far problem in the WPCN. Considering the near and far WDs from the HAP, we assign the far WDs a high priority and make them access at the later part of the frame in order to allow them to have a longer energy harvesting time than the near WDs. In terms of Jain's fairness index, we obtain the optimal ratio of RA slots allocated for the low- and high-priority WDs ($\alpha^*$) to maximize the fairness. Through an asymptotic analysis in the high signal-to-noise ratio (SNR) environment with a sufficient number of accessing WDs, it is shown that there are unique $m^*$ and $\alpha^*$ that maximize the channel throughput and user fairness, respectively, and both depend only on the average of the minimum SNRs of the WDs without the knowledge of full channel state information.

**INDEX TERMS** Wireless powered communication networks, wireless energy harvesting, slotted ALOHA, random access control, throughput maximization, priority, fairness.

## I. INTRODUCTION

The recent progress in radio frequency (RF)-based wireless energy transfer (WET) technology has resulted in the creation of a new networking structure called wireless powered communication networks (WPCNs), where wireless devices (WDs) replenish energy wirelessly from dedicated power transmitters and use it for wireless information transmission (WIT). Because the WPCN eliminates the need for manual battery replacement or recharge, it can effectively prolong the network lifetime, avoid energy outage of devices, and reduce the operation cost. Moreover, the WPCN can fully control both WET and WIT operations so that the transmit power, time/frequency, user scheduling, and antennas can all be controlled to match various network environments and service requirements for stable and on-demand energy supply [1], [2]. Therefore, many early studies on the WPCN are based on the centralized control, under which various types of radio resources are managed by a central coordinator (e.g., the hybrid access point (HAP)) to maximize performances [3]–[8].

In [3], the *harvest-then-transmit* protocol was proposed and the WET and WIT times were optimized under round-robin scheduling to maximize throughput. This harvest-then-transmit protocol was extended to the multi-antenna WPCN [5], full-duplex (FD) WPCN [6], FD WPCN with energy causality [7], and cooperative WPCN [8]. In [5], the downlink (DL) energy beamforming, uplink (UL) transmit power and receive beamforming, as well as WET/WIT time allocation, were jointly optimized to maximize the minimum throughput of all users. In [6], the WET/WIT time and the transmit power at the FD HAP were jointly optimized to maximize the weighted sum-rate. In [7], the WET/WIT time allocation was optimized to maximize the sum-rate or minimize the total transmission time under the energy

causality constraint. In [8], the WET/WIT time was optimized by considering the harvested energy from co-channel interferences among nearby users.

Such centralized approaches can achieve optimal performance in the WPCN, but require the global channel state information. This induces considerable signaling overhead for channel estimation and feedback and also high complexity for computation in proportion to the number of WDs. For this reason, most previous works have assumed that the HAP perfectly knows all channel information without overhead or considered a small number of users for optimization [3]–[8]. However, considering the current level of WET technology, which can transfer tens of microwatts of RF power to WDs from a distance of more than 10 m [9], the WPCN is potentially suitable for low-power applications with devices operating power up to several milliwatts, such as wireless sensor networks (WSNs) and RF identification networks. These applications generally support a large number of WDs and require to use a simple processor for low cost and energy saving. Therefore, it is difficult to maintain a centralized control in such practical WPCN environments so that a distributed protocol with low overhead and complexity needs to be designed.

Among the traditional random access protocols, slotted ALOHA operates in a simple distributed manner with low overhead and complexity and also offers many advantages, such as low delay to transmit a short packet, no initial connection setup, no pre-procedure before transmission, and no dedicated radio resource allocation for connection maintenance. Thus, it is more suitable than any other random access protocols when a large number of distributed nodes transmit data sporadically to the central node [10]. Therefore, we apply slotted ALOHA to the WPCN in this paper. Our main contributions are summarized as follows:

- We design a slotted ALOHA-based energy-harvesting medium access control (MAC) protocol for the WPCN. In this protocol, the WD randomly selects one of the given random access (RA) slots, continuously harvests the energy from the HAP until it has access, and then transmits data at the selected RA slot using the harvested energy.
- We perform an optimal resource allocation to maximize the throughput of the proposed protocol. To this end, we analyze the average channel throughput and derive the optimal number of RA slots to maximize it.
- To solve the *doubly near-far problem*[1] in WPCNs, we present a prioritized access control method in the proposed protocol. We divide the frame into two parts considering the near and far WDs from the HAP. Then, we assign the far WDs a high priority and make them access at the later part in order to allow them to have a longer EH time than the near WDs, which have a low priority and access at the front part.
- We analyze the user fairness considering the near and far WDs and derive the optimal allocation ratio of RA slots to maximize fairness. Considering Jain's fairness index as a function of the average throughputs of low- and high-priority WDs, we obtain the optimal ratio of RA slots allocated for the low- and high-priority WDs to maximize the fairness.

The rest of this paper is organized as follows. In Section II, we introduce the related distributed energy-harvesting MAC protocols. In Section III, we present the system model for the considered WPCN and explain the proposed protocol in detail. In Section IV, we analyze the average channel throughput and derive the optimal number of RA slots to maximize it. In Section V, the results for the optimal resource allocation are presented. In Section VI, we propose a prioritized access control method to alleviate the doubly near-far problem, analyze the user fairness, and derive the optimal ratio of resource allocated to low and high priorities for fairness maximization. In Section VII, we show the results for the prioritized access control. Finally, the concluding remarks are provided in Section VIII.

## II. RELATED WORKS

Distributed energy-harvesting MAC protocol is mainly divided into CSMA-based and ALOHA-based. In [11], an energy adaptive carrier sense multiple access (CSMA)-type MAC protocol was proposed, in which the access probability of a WD varies with its energy harvesting rate. In [12], the RF-MAC protocol was proposed, where multiple energy transmitters perform WET in respond to WDs' energy request and the energy harvesting WDs use a CSMA-based MAC protocol to coordinate the data exchange among one another. This RF-MAC requires the WDs to perform complicated computation and channel estimation tasks, and therefore a simplified version of RF-MAC was presented [13]. The throughput of RF-MAC was then analyzed with the energy queueing model [14]. Further, the harvest-then-transmit-based modified enhanced distributed coordination function (DCF) protocol was proposed by applying the IEEE 802.11e enhanced DCF to the harvest-then-transmit protocol, and optimization was performed to maximize the energy harvesting rate [15].

The performance of CSMA-based MAC protocols may deteriorate in dense networks with a large number of contending nodes because of its binary exponential backoff mechanism [16]. On the other hand, ALOHA-based MAC protocols have been applied to dense network environments with energy harvesting as an alternative distributed protocol. In [17], the throughput of slotted ALOHA protocol was analyzed in energy harvesting wireless networks. In [18], slotted ALOHA was applied to coordinate the transmission of data to a gateway in machine-to-machine (M2M) networks with energy harvesting, and the optimum sleep period was derived to keep the energy consumed in each device lower

[1]The doubly near-far problem occurs because far users from the HAP receive less wireless energy than near users in the DL but have to transmit with more power in the UL. Due to this problem, the throughput maximization approach severely degrades user fairness in the WPCN [3].

than the harvested energy. In [19] and [20], dynamic framed slotted ALOHA was analyzed in data collection networks with energy harvesting capabilities, and the MAC protocol and energy harvesting strategy were jointly optimized to prolong the network lifetime. However, these studies have not considered the WET from any dedicated energy transmitter as in WPCNs and assumed a fixed amount of energy arrival at random time instants from ambient energy sources. To the best of our knowledge, ALOHA-based protocols have never been applied to WPCNs.

## III. SYSTEM AND PROTOCOL

In this section, we first describe the system configurations and assumptions, and then explain the details of the proposed protocol.

### A. SYSTEM CONFIGURATIONS AND ASSUMPTIONS

We consider a WPCN cell with one HAP and $N$ WDs, as shown in figure 1. The HAP has a stable energy supply, but the WDs do not have any embedded energy sources. Thus, the HAP transfers energy wirelessly to all the WDs in the cell, and the WDs replenish energy from the HAP. The WDs then use the harvested energy to operate circuits and transmit UL data.

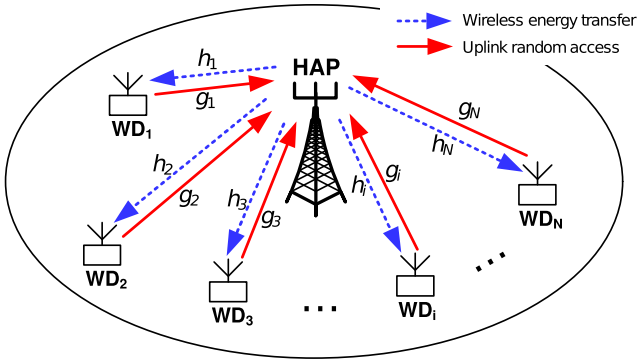


**FIGURE 1.** Considered wireless powered communication network.

Considering the low efficiency of WET technology, the WPCN is generally applicable to WSN or M2M network. In such applications, the WDs are usually regarded as low-power-consuming sensors with a small form factor. Thus, we suppose that the WDs store the harvested energy in a supercapacitor instead of a battery because the supercapacitor has the advantages of a small form factor, fast charging cycle, and many years of charging and discharging cycles, as compared to rechargeable batteries. However, supercapacitors suffer from high self-discharge and so may not be able to store the harvested energy long enough to be used for the next communication cycle [21]. To account for the high self-discharge characteristic of supercapacitors and the potential long delay between any two communication cycles in WSNs, we assume the WDs do not harvest energy after their transmission and transits to sleep mode until the next event occurs, In other words, it is beneficial for WDs with a supercapacitor to start energy harvesting when traffic occurs, rather than continuing energy harvesting while waiting for future traffic. These assumptions and system models are used in [7] and [22]–[24].

In addition, to achieve high spectral efficiency and efficient operation, we suppose that the HAP operates in FD mode so as to broadcast energy via DL WET and receive information via UL WIT at the same time [6], [7], [14]. The FD operation has become practical with the latest self-interference cancellation (SIC) technology, and because the efficiency of SIC is not the main focus in this study, we assume perfect SIC at the HAP [6], [7].[2] On the other hand, the WDs are assumed to operate in time-division half-duplex (HD) mode for low implementation cost so that they harvest energy in the DL and transmit data in the UL orthogonally over time.

### B. PROTOCOL DESIGN

When a large number of nodes generate traffic sporadically depending on the occurrence of an event, it is inappropriate to use the centralized access control, such as round-robin scheduling [3]–[8], so we consider a distributed access control by adapting a simple framed slotted ALOHA protocol [18]–[24]. Figure 2 shows the frame structure and the operation of the proposed protocol. Each frame consists of one beacon followed by multiple RA slots. At the beginning of every frame, the HAP broadcasts the beacon packet for frame synchronization and also to inform the WDs of the number of RA slots provided in a frame. During the period of RA slots, the FD HAP transfers energy wirelessly to the WDs and concurrently receives the UL data transmitted from them. On the other hand, the active WDs with the data to send randomly select one of the given RA slots, harvest the energy until they have access, and then transmit UL data at the selected RA slot using the harvested energy. After transmission, the WDs no longer continue harvesting energy and transit to sleep mode because the supercapacitor of WDs is subject to the high self-discharge property and it may take

[2]If the HAP operates in HD mode, two frequency bands for DL and UL are required for the proposed protocol. Even in this case, our formulation in Section IV is still valid by only the minor scaling of the pre-log factor.

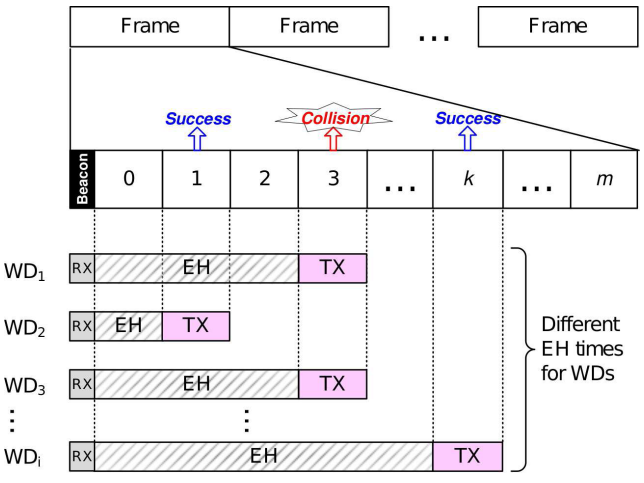


**FIGURE 2.** Frame structure and operation of proposed protocol.

a long time until the next data occurs [7], [22]–[24]. For this reason, the proposed protocol allows the WDs to have different EH times according to the position of the selected RA slot, unlike the previous harvest-then-transmit protocol that allocates the same EH time to all WDs before transmission. That is, later-transmitting WDs harvest more energy and this is consistent with the concept of energy causality addressed in [25]–[27]. Moreover, the WDs in the proposed protocol can harvest energy even in the idle slots where no one transmits data, while the typical slotted ALOHA and the harvest-then-transmit protocol cannot utilize the idle slots.

As shown in figure 2, in the proposed protocol, the first RA slot (i.e., slot 0) is dedicated to energy harvesting only to ensure that even the WD that selects the next RA slot (i.e., slot 1) can harvest the minimum energy for UL transmission [6]. Each frame provides $m$ RA slots available for UL transmission, and each WD performs a random access to one of the $m$ slots. Random access fails when two or more WDs select the same slot and succeeds when only one WD selects one slot, assuming that there is no channel error and capture effect [20].

## IV. OPTIMAL RESOURCE ALLOCATION FOR THROUGHPUT MAXIMIZATION

In this section, we analyze the average channel throughput of the proposed protocol and derive the optimal number of RA slots to maximize it.

### A. THROUGHPUT ANALYSIS

When an arbitrary WD$_i$ chooses the $k$-th slot for random access, its harvesting energy is expressed as

$$E_i^k = \zeta_i P h_i k T_s, \quad i \in \{1, 2, \cdots, N\}, \ k \in \{1, 2, \cdots, m\} \quad (1)$$

where $0 < \zeta_i < 1$ is the energy harvesting efficiency of WD$_i$, $P$ is the constant transmit power of HAP, $h_i$ is the channel power gain from the HAP to WD$_i$, and $T_s$ is the length of one RA slot. Then, the transmit power of WD$_i$ when it transmits data at the $k$-th RA slot is given by

$$P_i^k = \frac{\eta_i E_i^k}{T_s} = \eta_i \zeta_i P h_i k \quad (2)$$

where $0 < \eta_i < 1$ is the fraction of the harvested energy used by WD$_i$ to transmit its UL data.

If the WD$_i$'s random access at the $k$-th slot is successful, the achievable rate of WD$_i$ is calculated as

$$\begin{aligned} R_i^k &= \frac{T_s}{m T_s} \log_2 \left(1 + \frac{g_i P_i^k}{\Gamma \sigma^2}\right) \\ &= \frac{1}{m} \log_2 \left(1 + \frac{g_i \eta_i \zeta_i P h_i k}{\Gamma \sigma^2}\right) \\ &= \frac{1}{m} \log_2 (1 + \gamma_i k) \quad \text{[b/s/Hz]} \end{aligned} \quad (3)$$

where $g_i$ is the channel power gain from WD$_i$ to the HAP, $\Gamma$ represents the SNR gap, and $\sigma^2$ denotes the noise power at the HAP. Here, for the purpose of investigating the achievable maximum throughput, we assume that each WD has a sufficient amount of data to transmit during its selected slot duration and the HAP can estimate the uplink channel information $g_i$ by using a typical uplink channel estimation method [29]. In addition, $\gamma_i$ is defined as

$$\gamma_i \triangleq \frac{g_i \eta_i \zeta_i P h_i}{\Gamma \sigma^2}, \quad i \in \{1, 2, \cdots, N\} \quad (4)$$

Note that $\gamma_i$ is determined by the channel conditions and energy harvesting capability of WD$_i$ and so it is an independent parameter given to WD$_i$. We call $\gamma_i$ the *minimum* SNR ($m$SNR) of WD$_i$ at the HAP because $\gamma_i$ is the smallest SNR value that WD$_i$ can have when it selects the RA slot with $k = 1$. Note that as shown in (3), the actual SNR of WD$_i$ is jointly proportional to its $m$SNR $\gamma_i$ and the selected slot number $k$.

Let $\lambda$ be the average packet arrival rate at each WD in each frame. That is, each WD generates a packet to be sent with a probability of $\lambda$ every frame. Thus, we can suppose that $\lambda N$ WDs try to access $m$ RA slots every frame from the perspective of long-term average. In this case, the average successful access probability that only one WD accesses in a slot is given by

$$P_s = \lambda N \left(\frac{1}{m}\right) \left(1 - \frac{1}{m}\right)^{\lambda N - 1}. \quad (5)$$

Then, the average channel throughput (i.e., the average achievable rate of WDs during one frame) is calculated as

$$\begin{aligned} S &= \frac{1}{N} \sum_{i=1}^{N} \sum_{k=1}^{m} P_s R_i^k \\ &= \frac{\lambda}{m^2} \left(1 - \frac{1}{m}\right)^{\lambda N - 1} \sum_{k=1}^{m} \sum_{i=1}^{N} \log_2 (1 + \gamma_i k) \quad \text{[b/s/Hz]}. \end{aligned} \quad (6)$$

### B. THROUGHPUT MAXIMIZATION

The average channel throughput $S$ is a function of $m$ (i.e., the number of RA slots allocated) for given $N$, $\lambda$, and $\gamma_i$. To obtain the optimal $m$ analytically, we apply a high-SNR approximation (i.e., $\gamma_i k \geq \gamma_i \gg 1$) to (6). This is quite reasonable because the WPCN is suitable to high-SNR environments due to the low efficiency of practical WET technology [9], [28]. In addition, we apply the Poisson approximation (i.e., $\left(1 - \frac{1}{m}\right)^{\lambda N - 1} \approx e^{-\frac{\lambda N}{m}}$) assuming that the average number of accessing WDs is large enough (i.e., $\lambda N \gg 1$) [30]. Then, $S(m)$ is approximated as

$$\begin{aligned} \widetilde{S}(m) &= \frac{\lambda}{m^2} e^{-\frac{\lambda N}{m}} \sum_{k=1}^{m} \sum_{i=1}^{N} \log_2 (\gamma_i k) \\ &= \frac{\lambda}{m^2} e^{-\frac{\lambda N}{m}} \frac{1}{\ln 2} \left(m \sum_{i=1}^{N} \ln \gamma_i + N \sum_{k=1}^{m} \ln k\right) \\ &= \frac{\lambda N}{\ln 2} e^{-\frac{\lambda N}{m}} \left(\frac{1}{m} \frac{1}{N} \sum_{i=1}^{N} \ln \gamma_i + \frac{1}{m^2} \sum_{k=1}^{m} \ln k\right) \\ &= \frac{\lambda N}{\ln 2} e^{-\frac{\lambda N}{m}} \left(\frac{\bar{\gamma}}{m} + \frac{1}{m^2} \sum_{k=1}^{m} \ln k\right) \end{aligned} \quad (7)$$

where we define $\bar{\gamma} \triangleq \frac{1}{N}\sum_{i=1}^{N} \ln \gamma_i$, which corresponds to the average of the $m$SNRs of all the WDs in logarithmic scale. Using another approximation $\sum_{k=1}^{m} \ln k \approx \int_1^m \ln x dx = m \ln m - m + 1$ as a lower bound, the approximate average channel throughput $\widetilde{S}$ is expressed as

$$\begin{aligned}\widetilde{S}(m) &\approx \frac{\lambda N}{\ln 2} e^{-\frac{\lambda N}{m}} \left( \frac{\bar{\gamma}}{m} + \frac{m \ln m - m + 1}{m^2} \right) \\ &= \frac{\lambda N}{\ln 2} e^{-\frac{\lambda N}{m}} \frac{m(\ln m + (\bar{\gamma} - 1)) + 1}{m^2} \\ &= \frac{\lambda N}{\ln 2} e^{-\frac{\lambda N}{m}} \frac{m(\ln m + \bar{\gamma}') + 1}{m^2} \end{aligned} \tag{8}$$

where $\bar{\gamma}' \triangleq \bar{\gamma} - 1$ is defined.

Now we can find the optimal number of RA slots that maximizes the approximate average channel throughput given by (8).[3] The following lemma determines a unique solution of the optimal $m$.

*Lemma 1 (Solution of the Optimal $m$):* Let the optimal $m$ be $m^* = \arg_m \max \widetilde{S}(m)$. $m^*$ is then a unique solution of $f(m) = \bar{\gamma}$, where $f(m) = \frac{m-1}{m-\lambda N} - \frac{1}{m} - \ln m + 1$.

*Proof:* The derivative of $\widetilde{S}$ with respect to $m$ is given by

$$\begin{aligned}\frac{d\widetilde{S}}{dm} &= \frac{\lambda N}{\ln 2} e^{-\frac{\lambda N}{m}} \left\{ \frac{\lambda N}{m^2} \cdot \frac{m(\ln m + \bar{\gamma}') + 1}{m^2} \right. \\ &\quad \left. + \frac{m^2(\ln m + \bar{\gamma}' + 1) - 2m^2(\ln m + \bar{\gamma}') - 2m}{m^4} \right\} \\ &= \frac{\lambda N}{m^4 \ln 2} e^{-\frac{\lambda N}{m}} \left\{ \lambda N - m(2 - \lambda N(\ln m + \bar{\gamma}')) \right. \\ &\quad \left. - m^2(\ln m + \bar{\gamma}' - 1) \right\} \\ &= \frac{\lambda N}{m^4 \ln 2} e^{-\frac{\lambda N}{m}} \left\{ (\lambda N - m)(1 + (\ln m + \bar{\gamma}')m) \right. \\ &\quad \left. + m(m-1) \right\} \end{aligned} \tag{9}$$

where $\frac{d\widetilde{S}(m)}{dm} > 0$ is satisfied when $m \leq \lambda N$ because $\bar{\gamma}' > 0$ and $m > 1$. Moreover, the right-hand side of (9) can be expressed as $(\lambda N - m) + \left\{(\lambda N - m)(\ln m + \bar{\gamma}' - 1) + \lambda N\right\} m - m$. This is less than zero when $m \geq e\lambda N$ because $\bar{\gamma}' > 0$ and $\lambda N > 1$. That is, $\frac{d\widetilde{S}(m)}{dm} < 0$ is satisfied when $m \geq e\lambda N$. Thus, there is at least one $m^*$ that satisfies $\frac{d\widetilde{S}(m^*)}{dm} = 0$ in the range of $\lambda N < m^* < e\lambda N$.

From (9), the condition that satisfies $\frac{d\widetilde{S}(m)}{dm} = 0$ is given by

$$(\ln m + \bar{\gamma}')m = \frac{m(m-1)}{m - \lambda N} - 1 \tag{10}$$

$$\Leftrightarrow \bar{\gamma}' = \frac{m-1}{m-\lambda N} - \frac{1}{m} - \ln m \tag{11}$$

$$\Leftrightarrow \bar{\gamma} = \frac{m-1}{m-\lambda N} - \frac{1}{m} - \ln m + 1 \triangleq f(m) \tag{12}$$

where we define $f(m) \triangleq \frac{m-1}{m-\lambda N} - \frac{1}{m} - \ln m + 1$. Here, $\lim_{m \to \lambda N} f(m) = \infty$, $\lim_{m \to \infty} f(m) = -\infty$, and $f(m)$ is a monotonically decreasing function because $\frac{df(m)}{dm} = -\frac{\lambda N - 1}{(m-\lambda N)^2} - \frac{m-1}{m^2} < 0$ due to $\lambda N > 1$ and $m > 1$. Therefore, there exists a unique solution $m^*$ that satisfies $\frac{d\widetilde{S}(m^*)}{dm} = 0$ in the range of $\lambda N < m^* < e\lambda N$. This indicates that $\widetilde{S}(m)$ has a fundamental tradeoff with respect to $m$ because $\frac{d\widetilde{S}(m)}{dm} > 0$ for $m \leq \lambda N$ and $\frac{d\widetilde{S}(m)}{dm} < 0$ for $m \geq e\lambda N$. Finally, the optimal solution $m^*$ is calculated from

$$f(m^*) = \frac{m^* - 1}{m^* - \lambda N} - \frac{1}{m^*} - \ln m^* + 1 = \bar{\gamma}. \tag{13}$$

This completes the proof. ■

Because $m^*$ derived from Lemma 1 is a real value, we finally determine the value of $m^*$ as an integer as follows:

$$m^* = \begin{cases} \lceil m^* \rceil & \text{if } \widetilde{S}(\lceil m^* \rceil) > \widetilde{S}(\lfloor m^* \rfloor), \\ \lfloor m^* \rfloor & \text{otherwise.} \end{cases} \tag{14}$$

*Remark 1:* It is worth noting that the HAP only needs to know the value of $\bar{\gamma}$ (i.e., the average of the natural log of the $m$SNRs of all the WDs) for optimal resource allocation, without explicit knowledge of the individual channel of all the WDs. In practice, the value of $\bar{\gamma}$ can be estimated by gathering the $m$SNRs extracted from the successfully received signals of the WDs at the HAP from the perspective of the long-term average. This, in turn, significantly reduces the channel feedback overhead.

## V. RESULTS FOR OPTIMAL RESOURCE ALLOCATION

This section provides the analysis and simulation results of the proposed protocol using the optimal resource allocation. Table 1 summarizes the parameters used for the evaluation. We deploy a WPCN cell with a radius of 25 m and uniformly distribute 100 WDs in the cell considering the environments of high SNR and high density [31]. We then change the packet arrival rate $\lambda$ from 0.1 to 1 to control the number of accessing WDs in each frame. The transmit power of the HAP and the SNR gap are fixed as 40 dBm and 9.8 dB, respectively. Considering a practical WET level, the energy harvesting efficiency $\zeta_i$ is set to 0.5 for all $i$ [3]. Moreover, the fraction of harvested energy used for UL transmission $\eta_i$ is set to 0.8 for all $i$ considering the extra energy needed to operate the circuit.

**TABLE 1. Parameter setup.**

| Parameter | Value |
|---|---|
| Cell radius of WPCN | $r = 25$ m |
| Number of WDs in a cell | $N = 100$ |
| Packet arrival rate | $\lambda = 0.1 \sim 1.0$ |
| Transmit power of HAP | $P = 40$ dBm |
| SNR gap | $\Gamma = 9.8$ dB |
| Energy harvesting efficiency | $\zeta_i = 0.5\ \forall i$ |
| Fraction of harvested energy used for tx. | $\eta_i = 0.8\ \forall i$ |
| Noise spectral density at HAP | $-160$ dBm/Hz |
| Channel bandwidth | 1 MHz |
| Channel power gain | $h_i = g_i = G\rho_i^2 d_i^{-n}$ |
| Ave. power attenuation at a ref. dist. of 1 m | $G = -30$ dB |
| Channel fading | $\rho_i^2 \sim \text{Exp}(1)$ |
| Distance between HAP and WD$_i$ | $d_i = \text{Uniform}[1, 25]$ m |
| Path loss exponent | $n = 2 \sim 3$ (default=2.5) |
| Simulation trials | 10,000 |

[3] Such approximations are applied only for theoretical analysis and the impact of the applied approximations will be verified by numerical simulations in practical environments in Section V.

The noise spectral density at the HAP is set to $-160$ dBm/Hz, and the channel bandwidth is set to 1 MHz. For ease of exposition, we consider a simple distance-dependent path loss model given by $h_i = g_i = G\rho_i^2 d_i^{-n}$ under the assumptions that the DL and UL channels are reciprocal [14]. Here, $G$ refers to the average power attenuation at a reference distance of 1 m and is set to $-30$ dB [8], $\rho_i$ represents the additional short-term fading with Rayleigh distribution [3], $d_i$ is the distance between the HAP and a WD uniformly distributed between 1 and 25 m, and $n$ is the path loss exponent that varies between 2 (line-of-sight (LoS)) and 3 (non-LoS) and is set to 2.5 as default if not mentioned otherwise. It is assumed that both the DL and UL channels are quasi-static flat-fading, where $h_i$'s and $g_i$'s remain constant for each frame.

Throughout the results, we present two analysis results: one is the exact analysis in which the throughput is obtained from (6) without an approximation and the optimal $m^*$ is found by exhaustive search. The other is the approximate analysis in which the throughput is obtained from (8) and the optimal $m^*$ is calculated by (14). We also perform Monte Carlo simulations with 10,000 trials to validate these analysis results.

Figure 3 shows the average channel throughput versus the number of RA slots ($m$) when the packet arrival rate ($\lambda$) is set to 0.5 and 1, respectively. As $m$ increases, the channel throughput increases monotonically and then gradually decreases after a certain value of $m$. That is, there exists a unique optimal $m^*$ that maximizes the channel throughput in each $\lambda$, as proved in Lemma 1. When more WDs are accessing (i.e., at $\lambda = 1$), a larger $m^*$ is needed and a higher throughput is shown due to the longer EH time. The exact analysis results match the simulation results well. However, there is a slight difference between the exact and approximate analyses due to the high-SNR approximation used to obtain the approximate throughput.

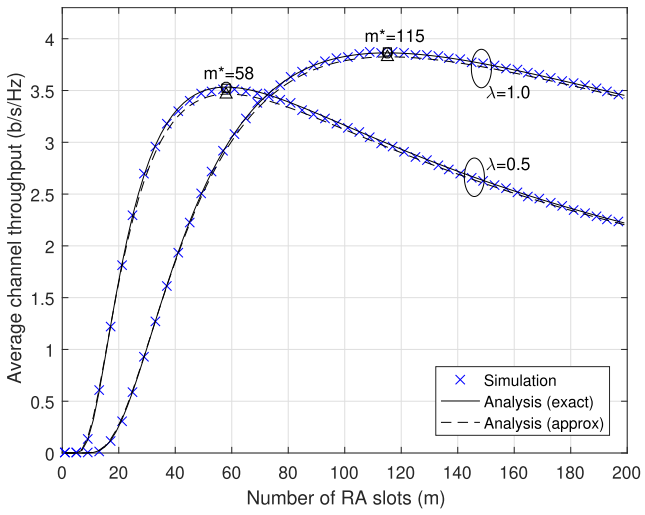


**FIGURE 3.** Average channel throughput vs. number of RA slots when $\lambda = 0.5$ and 1.

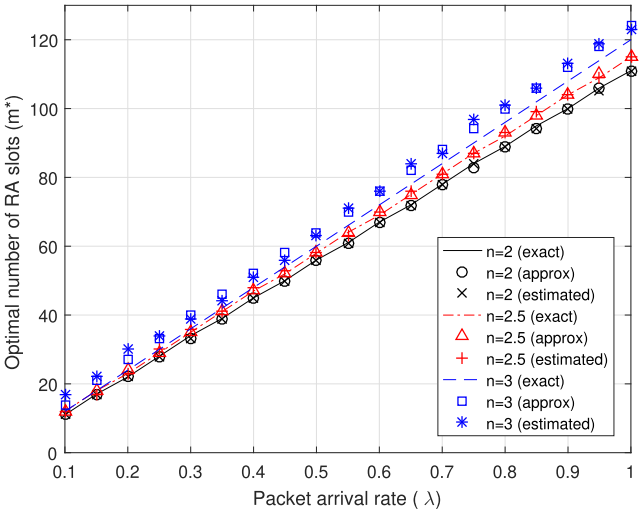


**FIGURE 4.** Optimal number of RA slots ($m^*$) vs. packet arrival rate according to path loss exponent ($n$).

Figure 4 shows the optimal number of RA slots ($m^*$) versus the packet arrival rate ($\lambda$) for different values of the path loss exponent ($n$). It is observed that the optimal $m^*$ linearly increases as $\lambda$ increases (i.e., the number of accessing WDs increases). In addition, the optimal $m^*$ increases as the path loss exponent increases. This is because the higher path loss exponent reduces the SNR of WDs, and thus they require a higher transmission power (i.e., a longer EH time) to compensate for it and maintain the throughput. From Lemma 1, we can also understand that the optimal $m^*$ satisfying $f(m^*) = \bar{\gamma}$ increases as the average $m$SNRs $\bar{\gamma}$ is decreased by the higher path loss exponent because $f(m)$ is a decreasing function. When the path loss exponent is greater than 2.5, the difference between the exact and approximate analysis begins to emerge, because the high-SNR approximation does not fit well from this point. Additionally, we investigate the effect of the estimated $\bar{\gamma}$ on the optimal $m^*$ from the practical point of view. Since the access of the WDs may be collided, it takes time to compile all the WD's $\gamma$ values, as mentioned in Remark 1. Thus, there might be an error between the estimated $\bar{\gamma}$ and the actual $\bar{\gamma}$. However, we can observe that there is no significant difference in the optimal $m^*$ when we use $\bar{\gamma}$ estimated for four frames.

Figure 5 shows the average channel throughput versus the packet arrival rate. When the fixed $m$ is used, the throughput increases and then decreases with increasing $\lambda$ because the number of offered RA slots does not adapt to the number of accessing WDs. However, when the optimal $m$ is used, the throughput always maintains peak values regardless of $\lambda$. It is shown that there is little difference among the uses of the exact $m^*$, approximate $m^*$, and $m^*$ obtained from the estimated $\bar{\gamma}$, in terms of the throughput. Moreover, we compare the proposed protocol with the competitive harvest-then-transmit-based slotted ALOHA protocol [20]. This harvest-then-transmit-based slotted ALOHA protocol allocates a separate fixed EH time to all WDs at the beginning of

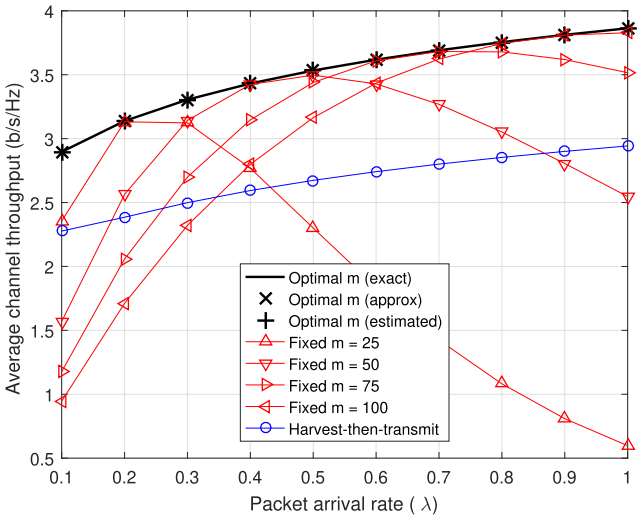


**FIGURE 5.** Average channel throughput vs. packet arrival rate.

the frame and then attempts random access based on slotted ALOHA after harvesting, unlike the proposed protocol allows the WDs to have different EH times. Here, the length of EH time is optimized by exhaustive search to maximize throughput for a fair comparison with proposed method. As shown, the harvest-then-transmit-based slotted ALOHA has significantly lower throughput than the proposed protocol. This is because it uses a separate additional EH time and also there exist the idle slots that are not used for any purpose during the RA period.

## VI. PRIORITIZED ACCESS CONTROL FOR FAIRNESS MAXIMIZATION

To tackle the doubly near-far problem in the WPCN, we present a prioritized access control method in the proposed protocol. After presenting the motivation and basic operation of the method, we analyze user fairness considering two priorities and derive the optimal allocation ratio of RA slots for each priority to maximize fairness.

### A. MOTIVATION AND OPERATION

The WPCN suffers from the doubly near-far problem that is caused by the double signal attenuation in both the DL and the UL. Due to this problem, the throughput maximization approach significantly degrades user fairness [3], [6]. Similarly, the throughput maximization solution in the previous section also degrades user fairness. That is, near WDs from the HAP experience a much higher throughput than far WDs from the HAP.[4] By the way, in the proposed protocol, a node that selects a larger RA slot number has a longer EH time than another node that selects a smaller number. Therefore, if we make the near WDs access the earlier slots in the frame and the far WDs access the later slots in the frame, the near/far WDs can use lower/higher transmission power than when accessing in the entire slot area. This can reduce the difference in throughput between near and far WDs so that the doubly near-far problem is alleviated.

To realize this concept, we develop a prioritized access control, where the entire RA slot is divided into two parts considering two priority groups of the near and far WDs, as shown in figure 6. To give more opportunity for the far WDs to harvest more energy before access, we give high priority to the WDs with low $m$SNR (i.e., far WDs) and make them access the second RA slot area. On the contrary, the WDs with high $m$SNR (i.e., near WDs) have a low priority and access the first RA slot area. Specifically, the WDs that satisfy $\ln \gamma_i \geq \bar{\gamma}$ (i.e., if its $m$SNR is greater than or equal to the average $m$SNR of all WDs in logarithmic scale) become the low-priority WD, and the other WDs that satisfy $\ln \gamma_i < \bar{\gamma}$ become the high-priority WD.[5] Thus, each WD needs to know both values of $\gamma_i$ and $\bar{\gamma}$ to determine its priority. Since $\bar{\gamma}$ is measured in the HAP, the HAP should inform the value of $\bar{\gamma}$ to WDs through the beacon message at the beginning of every frame. In addition, the WDs can estimate its $\gamma_i$ while receiving the beacon message assuming that DL and UL channels are reciprocal [14]. Specifically, it can be estimated by $\gamma_i = \widetilde{h}_i \eta_i \zeta_i \gamma_i'$ where $\gamma_i'$ is the SNR received at the WD$_i$ given by $\gamma_i' = \frac{P h_i}{\Gamma \sigma^2}$ and $\widetilde{h}_i$ is the estimated DL channel from the HAP to WD$_i$.

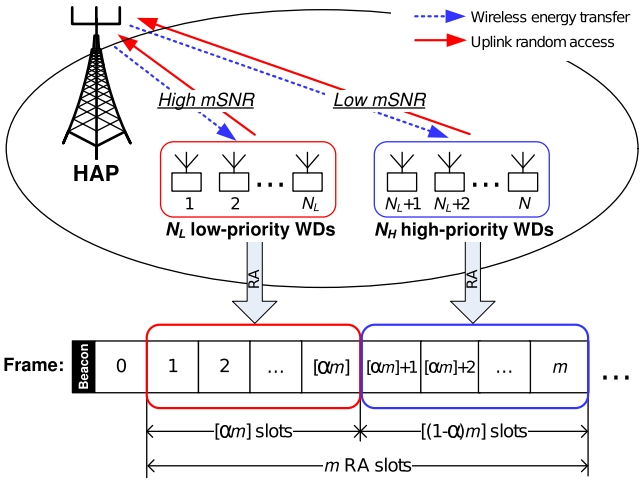


**FIGURE 6.** Prioritized access control considering near and far WDs.

According to these criteria of dividing priority, the total $N$ WDs is divided into $N_L$ low-priority WDs and $N_H$ high-priority WDs (i.e., $N_L + N_H = N$). Moreover, we suppose that among the total $m$ RA slots given, $m_L$ slots are allocated to the low-priority WDs and $m_H$ slots are allocated to the high-priority WDs (i.e., $m_L + m_H = m$). Then, there remains only the matter of deciding how to divide the entire slot for each priority. By applying a ratio $0 < \alpha < 1$, we set

[4]This phenomenon will be shown in figure 9(b).

[5]Note that $\bar{\gamma}$ is a representative parameter indicating the average channel state of all WDs managed by the HAP for optimal resource allocation, as mentioned in Remark 1. Thus, we can easily apply it to distinguish WDs. Through experiments in various environments, we have confirmed that this criterion is well suited for dividing near WDs and far WDs.

$m_L = [\alpha m]$ and $m_H = [(1-\alpha)m]$, where $[x]$ is a function that returns the nearest integer to $x$. Thus, our objective is to find the optimal $\alpha$ to maximize user fairness by considering two priorities of near and far WDs in order to solve the doubly near-far problem.[6]

### B. FAIRNESS ANALYSIS

First, we analyze user fairness. When $\lambda N$ WDs try to access $m$ RA slots in each frame, the average throughput of WD$_i$ is obtained from (3) and (5), as follows:

$$\begin{aligned} U_i &= \frac{1}{N}\sum_{k=1}^{m} P_s R_i^k \\ &= \frac{\lambda}{m}\left(1-\frac{1}{m}\right)^{\lambda N-1}\sum_{k=1}^{m}\log_2\left(1+\gamma_i k\right), \\ &\qquad i \in \{1,2,\cdots,N\}. \end{aligned} \tag{15}$$

Without loss of generality, we suppose that WD$_i$ for $i \in \{1,2,\cdots,N_L\}$ has low priority and WD$_i$ for $i \in \{N_L+1, N_L+2,\cdots,N\}$ has high priority, subject to $N_L+N_H=N$. When $N_L$ low-priority WDs access the first $m_L$ slots and $N_H$ high-priority WDs access the later $m_H$ slots, the average throughputs of low- and high-priority WD$_i$ are respectively expressed as

$$\begin{aligned} U_i^L(\alpha) &= \frac{1}{N_L}\sum_{k=1}^{m_L} P_s R_i^k \\ &= \frac{\lambda}{m_L}\left(1-\frac{1}{m_L}\right)^{\lambda N_L-1}\sum_{k=1}^{m_L}\log_2\left(1+\gamma_i k\right), \\ &\qquad i \in \{1,2,\cdots,N_L\}. \end{aligned} \tag{16}$$

$$\begin{aligned} U_i^H(\alpha) &= \frac{1}{N_H}\sum_{k=m_L+1}^{m} P_s R_i^k \\ &= \frac{\lambda}{m_H}\left(1-\frac{1}{m_H}\right)^{\lambda N_H-1}\sum_{k=m-m_H+1}^{m}\log_2\left(1+\gamma_i k\right), \\ &\qquad i \in \{N_L+1, N_L+2,\cdots,N\}. \end{aligned} \tag{17}$$

Similar to (7) and (8), $U_i^L$ for $i \in \{1,2,\cdots,N_L\}$ is approximated as

$$\begin{aligned} \widetilde{U}_i^L(\alpha) &= \frac{\lambda}{m_L}e^{-\frac{\lambda N_L}{m_L}}\sum_{k=1}^{m_L}\log_2(\gamma_i k) \\ &= \frac{\lambda}{m_L}e^{-\frac{\lambda N_L}{m_L}}\frac{1}{\ln 2}\left(m_L\ln\gamma_i+\sum_{k=1}^{m_L}\ln k\right) \\ &= \frac{\lambda}{\ln 2}e^{-\frac{\lambda N_L}{m_L}}\left(\ln\gamma_i+\frac{1}{m_L}\sum_{k=1}^{m_L}\ln k\right) \\ &\overset{(a)}{\approx} \frac{\lambda}{\ln 2}e^{-\frac{\lambda N_L}{\alpha m}}\left(\ln\gamma_i+\frac{1}{\alpha m}\int_1^{\alpha m}\ln x dx\right) \\ &= \frac{\lambda}{\ln 2}e^{-\frac{\lambda N_L}{\alpha m}}\left(\ln\gamma_i+\frac{\alpha m\ln\alpha m-\alpha m+1}{\alpha m}\right) \\ &= \frac{\lambda}{\ln 2}e^{-\frac{\lambda N_L}{\alpha m}}\left(\ln\gamma_i+\ln m-1+\ln\alpha+\frac{1}{\alpha m}\right) \end{aligned} \tag{18}$$

where (a) comes from $\sum_{k=1}^{m_L}\ln k \approx \int_1^{m_L}\ln x dx \approx \int_1^{\alpha m}\ln x dx$. In addition, $U_i^H$ for $i \in \{N_L+1, N_L+2,\cdots,N\}$ is approximated as

$$\begin{aligned} &\widetilde{U}_i^H(\alpha) \\ &= \frac{\lambda}{m_H}e^{-\frac{\lambda N_H}{m_H}}\sum_{k=m-m_H+1}^{m}\log_2(\gamma_i k) \\ &= \frac{\lambda}{m_H}e^{-\frac{\lambda N_H}{m_H}}\frac{1}{\ln 2}\left(m_H\ln\gamma_i+\sum_{k=m-m_H+1}^{m}\ln k\right) \\ &= \frac{\lambda}{\ln 2}e^{-\frac{\lambda N_H}{m_H}}\left(\ln\gamma_i+\frac{1}{m_H}\sum_{k=m-m_H+1}^{m}\ln k\right) \\ &\overset{(b)}{\approx} \frac{\lambda}{\ln 2}e^{-\frac{\lambda N_H}{(1-\alpha)m}}\left(\ln\gamma_i+\frac{1}{(1-\alpha)m}\int_{\alpha m}^{m}\ln x dx\right) \\ &= \frac{\lambda}{\ln 2}e^{-\frac{\lambda N_H}{(1-\alpha)m}}\left\{\ln\gamma_i+\frac{m\ln m-m-\alpha m\ln(\alpha m)+\alpha m}{(1-\alpha)m}\right\} \\ &= \frac{\lambda}{\ln 2}e^{-\frac{\lambda N_H}{(1-\alpha)m}}\left(\ln\gamma_i+\ln m-1-\frac{\alpha}{1-\alpha}\ln\alpha\right) \end{aligned} \tag{19}$$

where (b) comes from $\sum_{k=m-m_H+1}^{m}\ln k \approx \int_{m-m_H+1}^{m}\ln x dx \approx \int_{\alpha m}^{m}\ln x dx$.

To evaluate user fairness, we adopt Jain's fairness index [32], which is formulated as

$$\begin{aligned} &\mathcal{J}(U_1,U_2,\cdots,U_N) \\ &\triangleq \frac{\left(\sum_{i=1}^{N}U_i\right)^2}{N\sum_{i=1}^{N}(U_i)^2} \\ &= \frac{\left(\sum_{i=1}^{N_L}U_i^L(\alpha)+\sum_{i=N_L+1}^{N}U_i^H(\alpha)\right)^2}{(N_L+N_H)\left\{\sum_{i=1}^{N_L}(U_i^L(\alpha))^2+\sum_{i=N_L+1}^{N}(U_i^H(\alpha))^2\right\}} \\ &\approx \frac{\left(\sum_{i=1}^{N_L}\widetilde{U}_i^L(\alpha)+\sum_{i=N_L+1}^{N}\widetilde{U}_i^H(\alpha)\right)^2}{(N_L+N_H)\left\{\sum_{i=1}^{N_L}(\widetilde{U}_i^L(\alpha))^2+\sum_{i=N_L+1}^{N}(\widetilde{U}_i^H(\alpha))^2\right\}}. \end{aligned} \tag{20, 21}$$

This Jain's fairness index has a maximum value of one when $U_i$ is identical for $\forall i \in \{1,2,\cdots,N\}$. By the way, both $\widetilde{U}_i^L$ and $\widetilde{U}_i^H$ are functions of $\gamma_i$, and $\gamma_i$ is a different constant given by the channel condition and energy harvesting capability of each WD. Thus, for any given $\alpha$ and $m$, we cannot make $\widetilde{U}_i^L = \widetilde{U}_j^L$ for $\forall i,j \in \{1,2,\cdots,N_L\}, i \neq j$ and $\widetilde{U}_i^H = \widetilde{U}_j^H$ for $\forall i,j \in \{N_L+1, N_L+2,\cdots,N\}, i \neq j$, respectively, as long as $\gamma_i \neq \gamma_j$. Thus, as an alternative approach, we take into account the averages of $\widetilde{U}_i^L$ and $\widetilde{U}_i^H$ (i.e., the average user throughput in each priority) and equalize them by controlling $\alpha$ in the average sense.

[6] Considering only two priority levels facilitates the numerical analysis and optimization, but the extension to multiple priority levels is also possible in the same context. This is left as future work.

The average throughputs of low- and high-priority WDs are respectively calculated as

$$\begin{aligned}\bar{U}^L(\alpha) &= \frac{1}{N_L}\sum_{i=1}^{N_L}\widetilde{U}_i^L(\alpha)\\ &= \frac{\lambda}{\ln 2}e^{-\frac{\lambda N_L}{\alpha m}}\left(\frac{1}{N_L}\sum_{i=1}^{N_L}\ln\gamma_i+\ln m-1+\ln\alpha+\frac{1}{\alpha m}\right)\\ &= \frac{\lambda}{\ln 2}e^{-\frac{\lambda N_L}{\alpha m}}\left(\bar{\gamma}_L+\ln m-1+\ln\alpha+\frac{1}{\alpha m}\right), \qquad (22)\\ \bar{U}^H(\alpha) &= \frac{1}{N_H}\sum_{i=N_L+1}^{N}\widetilde{U}_i^H(\alpha)\\ &= \frac{\lambda}{\ln 2}e^{-\frac{\lambda N_H}{(1-\alpha)m}}\left(\frac{1}{N_H}\sum_{i=N_L+1}^{N}\ln\gamma_i+\ln m\right.\\ &\quad\left.-1-\frac{\alpha}{1-\alpha}\ln\alpha\right)\\ &= \frac{\lambda}{\ln 2}e^{-\frac{\lambda N_H}{(1-\alpha)m}}\left(\bar{\gamma}_H+\ln m-1-\frac{\alpha}{1-\alpha}\ln\alpha\right)\end{aligned} \qquad (23)$$

where $\bar{\gamma}_L \triangleq \frac{1}{N_L}\sum_{i=1}^{N_L}\ln\gamma_i$ and $\bar{\gamma}_H \triangleq \frac{1}{N_H}\sum_{i=N_L+1}^{N}\ln\gamma_i$ are defined, which correspond to the average of the $m$SNRs of low- and high-priority WDs in the logarithmic scale, respectively. From (21), by letting $\widetilde{U}_i^L = \bar{U}^L$ and $\widetilde{U}_i^H = \bar{U}^H$, Jain's fairness index for the average user throughput in each priority is reexpressed as

$$\mathcal{J}(\bar{U}^L,\bar{U}^H) = \frac{\left(N_L\bar{U}^L(\alpha)+N_H\bar{U}^H(\alpha)\right)^2}{(N_L+N_H)\left\{N_L(\bar{U}^L(\alpha))^2+N_H(\bar{U}^H(\alpha))^2\right\}}. \qquad (24)$$

This Jain's fairness index corresponds to the upper bound of the original Jain's fairness index given by (21), which is verified by the following Proposition 1.

*Proposition 1:* Let $\mathbf{x}$ and $\mathbf{y}$ be column vectors with all components non-negative in $\mathbb{R}^m$ and $\mathbb{R}^n$, respectively, for $m, n \geq 1$. The means of the $\mathbf{x}$ and $\mathbf{y}$ vectors are given by $\mu_x = \frac{1}{m}\mathbf{1}_m^T\mathbf{x}$ and $\mu_y = \frac{1}{n}\mathbf{1}_n^T\mathbf{y}$, respectively. Jain's fairness index is defined as

$$\mathcal{J}(\mathbf{x},\mathbf{y}) = \frac{(\sum_{i=1}^m x_i+\sum_{j=1}^n y_j)^2}{(m+n)(\sum_{i=1}^m x_i^2+\sum_{j=1}^n y^2)}. \qquad (25)$$

It then follows that $\mathcal{J}(\mathbf{x},\mathbf{y}) \leq \mathcal{J}(\bar{\mathbf{x}},\bar{\mathbf{y}})$ where $\bar{\mathbf{x}} = \mu_x\mathbf{1}_m$ and $\bar{\mathbf{y}} = \mu_y\mathbf{1}_n$.

*Proof:* Please refer to Appendix. ■

### C. FAIRNESS MAXIMIZATION

Now, we find the optimal $\alpha$ that maximizes $\mathcal{J}(\bar{U}^L,\bar{U}^H)$ as the upper bound of $\mathcal{J}(U_i^L,U_i^H)$, which is expressed as

$$\alpha^* = \arg_\alpha\max\mathcal{J}(\bar{U}^L,\bar{U}^H). \qquad (26)$$

Note that the difference between this approximate $\alpha^*$ and the exact $\alpha^* = \arg_\alpha\max\mathcal{J}(U_i^L,U_i^H)$ will be verified by numerical simulations in Section VII. Because $\mathcal{J}(\bar{U}^L,\bar{U}^H)$ is maximized when $\bar{U}^L(\alpha) = \bar{U}^H(\alpha)$, we can obtain the optimal $\alpha$ satisfying the following relationship from (22) and (23):

$$\begin{aligned}&e^{-\frac{\lambda N_L}{\alpha m}}\left\{\bar{\gamma}_L+\ln m-1+\ln\alpha+\frac{1}{\alpha m}\right\}\\ &\quad= e^{-\frac{\lambda N_H}{(1-\alpha)m}}\left\{\bar{\gamma}_H+\ln m-1-\frac{\alpha}{1-\alpha}\ln\alpha\right\}.\end{aligned} \qquad (27)$$

The following two lemmas explain that there exists a unique solution of the optimal $\alpha$ satisfying (27).

*Lemma 2 (Existence of the Optimal $\alpha$):* Let $f_1(\alpha) = e^{-\frac{\lambda N_L}{\alpha m}}(\bar{\gamma}_L+\ln m-1+\ln\alpha+\frac{1}{\alpha m})$ and $f_2(\alpha) = e^{-\frac{\lambda N_H}{(1-\alpha)m}}(\bar{\gamma}_H+\ln m-1-\frac{\alpha}{1-\alpha}\ln\alpha)$ with any given $\bar{\gamma}_L,\bar{\gamma}_H,m>1$. There then exists at least one solution $\alpha^*$ such that $f_1(\alpha^*) = f_2(\alpha^*)$ for $\alpha^*\in(0,1)$.

*Proof:* Both $f_1(\alpha)$ and $f_2(\alpha)$ are continuous functions for $\alpha\in(0,1)$ because both are differentiable with respect to $\alpha$. When $\alpha$ approaches 0 or 1, $f_1(\alpha)$ and $f_2(\alpha)$ approach as follows:

$$\lim_{\alpha\to0}f_1(\alpha) = 0, \qquad (28)$$

$$\lim_{\alpha\to1}f_1(\alpha) = e^{-\frac{\lambda N_L}{m}}(\bar{\gamma}_L+\ln m-1+\frac{1}{m}) > 0, \qquad (29)$$

$$\lim_{\alpha\to0}f_2(\alpha) = (\bar{\gamma}_H+\ln m-1)e^{-\frac{\lambda N_H}{m}} > 0, \qquad (30)$$

$$\lim_{\alpha\to1}f_2(\alpha) = 0 \qquad (31)$$

which can be obtained by L'Hopital's rule. Because $\lim_{\alpha\to0}f_1(\alpha) < \lim_{\alpha\to0}f_2(\alpha)$ and $\lim_{\alpha\to1}f_1(\alpha) > \lim_{\alpha\to1}f_2(\alpha)$ are established, there exists at least one intersection of $f_1(\alpha)$ and $f_2(\alpha)$ where $\alpha\in(0,1)$. This completes the proof. ■

*Lemma 3 (Uniqueness of the Optimal $\alpha$):* There exists a unique solution $\alpha^*$ such that $f_1(\alpha^*) = f_2(\alpha^*)$ for $\alpha^*\in(0,1)$ if the condition $\bar{\gamma}_H+\ln m-1 \gg \frac{m}{\lambda N_H}$ is satisfied.

*Proof:* The derivative of $f_1(\alpha)$ with respect to $\alpha$ is given by

$$\begin{aligned}\frac{\partial f_1(\alpha)}{\partial\alpha} &= e^{-\frac{\lambda N_L}{\alpha m}}\left(\frac{\lambda N_L}{m\alpha^2}\right)\left(\bar{\gamma}_L+\ln m-1+\ln\alpha+\frac{1}{\alpha m}\right)\\ &\quad+e^{-\frac{\lambda N_L}{\alpha m}}\left(\frac{1}{\alpha}-\frac{1}{m\alpha^2}\right)\\ &= e^{-\frac{\lambda N_L}{\alpha m}}\left(\frac{\lambda N_L}{m\alpha^2}\right)\left\{\ln(\alpha m)+\frac{1}{\alpha m}-1\right\}\\ &\quad+e^{-\frac{\lambda N_L}{\alpha m}}\left\{\frac{1}{m\alpha^2}(\lambda N_L\bar{\gamma}_L-1)+\frac{1}{\alpha}\right\}\end{aligned} \qquad (32)$$

where we define $g(\alpha) \triangleq \ln(\alpha m)+\frac{1}{\alpha m}-1$. Then, $g(\alpha)\geq0$ for $\alpha\in(0,1)$ because $g(\frac{1}{m}) = 0$, $\frac{\partial g(\alpha)}{\partial\alpha} = \frac{1}{\alpha}\left(1-\frac{1}{\alpha m}\right) < 0$ for $\alpha < \frac{1}{m}$, and $\frac{\partial g(\alpha)}{\partial\alpha} > 0$ for $\alpha > \frac{1}{m}$. Moreover, $\lambda N_L\bar{\gamma}_L-1\geq0$ because $\lambda N_L \geq 1$ (i.e., at least one user is accessing) and $\bar{\gamma}_L > 1$. Therefore, $\frac{\partial f_1(\alpha)}{\partial\alpha} > 0$ is satisfied so that $f_1(\alpha)$ is a monotonic increasing function for $\alpha\in(0,1)$.

In addition, the derivative of $f_2(\alpha)$ with respect to $\alpha$ is written as

$$\begin{aligned}
&\frac{\partial f_2(\alpha)}{\partial \alpha} \\
&= e^{-\frac{\lambda N_H}{(1-\alpha)m}} \frac{-\lambda N_H}{(1-\alpha)^2 m}\left(\bar{\gamma}_H + \ln m - 1 - \frac{\alpha}{1-\alpha}\ln\alpha\right) \\
&\quad + e^{-\frac{\lambda N_H}{(1-\alpha)m}}\left(\frac{-1}{(1-\alpha)^2}\ln\alpha - \frac{1}{1-\alpha}\right) \\
&= e^{-\frac{\lambda N_H}{(1-\alpha)m}}\left\{\frac{\lambda N_H}{(1-\alpha)^2 m}\left(-(\bar{\gamma}_H + \ln m - 1) + \frac{\alpha}{1-\alpha}\ln\alpha\right)\right. \\
&\quad \left. + \frac{\alpha - \ln\alpha - 1}{(1-\alpha)^2}\right\} \\
&= e^{-\frac{\lambda N_H}{(1-\alpha)m}} \frac{\lambda N_H}{(1-\alpha)^2 m}\{-(\bar{\gamma}_H + \ln m - 1) \\
&\quad + \frac{\alpha}{1-\alpha}\ln\alpha + \frac{m}{\lambda N_H}(\alpha - \ln\alpha - 1)\}
\end{aligned} \tag{33}$$

where we define $h(\alpha) \triangleq -k_1 + \frac{\alpha}{1-\alpha}\ln\alpha + k_2(\alpha - \ln\alpha - 1)$ by letting $k_1 = \bar{\gamma}_H + \ln m - 1$ and $k_2 = \frac{m}{\lambda N_H}$. Applying the relation $\frac{\alpha^2-1}{2\alpha} \le \ln\alpha \le \frac{2(\alpha-1)}{1+\alpha}$ to $h(\alpha)$, it is formulated as [33]

$$\begin{aligned}
h(\alpha) &\le -k_1 + \frac{\alpha}{1-\alpha}\cdot\frac{2(\alpha-1)}{1+\alpha} + k_2\left(\alpha - \frac{\alpha^2-1}{2\alpha} - 1\right) \\
&= \frac{k_2}{2\alpha(1+\alpha)}\left(\alpha^3 - \frac{2k_1+k_2+4}{k_2}\alpha^2 - \frac{2k_1+k_2}{k_2}\alpha + 1\right) \\
&\le \frac{k_2}{2\alpha(1+\alpha)}\left(\alpha^3 - \omega\alpha^2 - \omega\alpha + 1\right), \quad \omega \triangleq \frac{2k_1}{k_2} + 1 > 0 \\
&= \frac{k_2}{2\alpha}\left(\alpha - \underbrace{\frac{\omega + 1 - \sqrt{(\omega+1)^2 - 4}}{2}}_{\to 0 \text{ if } \omega \gg 1}\right) \\
&\quad \cdot \left(\alpha - \underbrace{\frac{\omega + 1 + \sqrt{(\omega+1)^2 - 4}}{2}}_{\to(\omega+1) \text{ if } \omega \gg 1}\right) \\
&= \frac{k_2}{2}(\alpha - \omega - 1) \text{ if } \omega \gg 1 \\
&< 0 \ (\because 0 < \alpha < 1 \text{ and } \omega > 0).
\end{aligned} \tag{34}$$

If $\omega \gg 1$, $h(\alpha) < 0$ and thus $\frac{\partial f_2(\alpha)}{\partial \alpha} < 0$ is satisfied because the first term in (33), $e^{-\frac{\lambda N_H}{(1-\alpha)m}}\frac{\lambda N_H}{(1-\alpha)^2 m}$, is non-negative. Therefore, $f_2(\alpha)$ is a monotonic decreasing function for $\alpha \in (0, 1)$ when $\omega \gg 1$, which is equivalent to $k_1 \gg k_2$ by definition; that is, $\bar{\gamma}_H + \ln m - 1 \gg \frac{m}{\lambda N_H}$. Under this condition, $f_1(\alpha)$ and $f_2(\alpha)$ intersect at only one point where $\alpha \in (0, 1)$. This completes the proof. ■

On the basis of the Lemmas 2 and 3, the optimal $\alpha^*$ satisfying (27) can be easily found by using a numerical method (e.g., the bisection method).

*Remark 2:* It is worth noting that we have confirmed through numerical simulations that the condition $\bar{\gamma}_H + \ln m - 1 \gg \frac{m}{\lambda N_H}$ is always satisfied in the considered WPCN environments with sufficient WDs and a high SNR (i.e., with the parameters of $N = 100$, $\lambda = 0.1 \sim 1$, $n = 2 \sim 3$, etc., as shown in Table 1). Therefore, we can find the unique $\alpha^*$ satisfying $f_1(\alpha^*) = f_2(\alpha^*)$ in the considered WPCN environments. This result will be shown in figure 8 in Section VII.

*Remark 3:* Similar to Remark 1, the HAP only needs to know the values of $\bar{\gamma}_L$ and $\bar{\gamma}_H$ to obtain the optimal allocation ratio $\alpha^*$, without explicit knowledge of the channel information of each WD. Likewise, this requirement significantly reduces system overhead and complexity.

## VII. RESULTS FOR PRIORITIZED ACCESS CONTROL

This section provides the analysis and simulation results for the proposed prioritized access control. We use the same parameters as shown in Table 1. In addition, we set the total number of RA slots used in the prioritized access control to the optimal $m^*$ derived from (14) for throughput maximization, in order to compare the proposed scheme with the no-priority scheme with maximum channel throughput. Similarly, we present two analysis results: one is the exact analysis in which the fairness is calculated by (20) without approximation and the optimal $\alpha^*$ that maximizes (20) is found by exhaustive search. The other is the approximate analysis in which the fairness is calculated by (24) and the optimal $\alpha^*$ is obtained from (27).

Figure 7 shows the average user throughput of low- and high-priority WDs and Jain's fairness index versus the allocation ratio of RA slots for each priority ($\alpha$) when $\lambda = 1$. As $\alpha$ increases, the throughput of low-priority WDs increases, but the throughput of high-priority WDs decreases. Accordingly, there exists a unique $\alpha^*$ that makes the throughputs of the two priorities equal and also the fairness has a maximum at this $\alpha^*$. In this case, $N_L = 40$ and $N_H = 60$ are determined by the criterion of dividing the priority user, but the optimal $\alpha^* = 0.25 < \frac{40}{40+60}$ is derived. This means that a lot more RA slots should be allocated to the high-priority WDs to provide them with longer EH time and more successful access considering their poor channel conditions. In terms of the average user throughput, the simulation, exact analysis, and approximate analysis exhibit close agreement. However, the approximate fairness is slightly higher than the exact fairness because it is the upper bound of the exact fairness. Nevertheless, the optimal $\alpha^*$ derived from the approximate analysis is almost the same as the optimal $\alpha^*$ obtained by the exact analysis and simulation.

Figure 8 shows the optimal allocation ratio ($\alpha^*$) versus the packet arrival rate ($\lambda$) for different values of the path loss exponent ($n$). The optimal $\alpha^*$ decreases as the path loss exponent increases. This is because as the path loss exponent increases, the SNR of far WDs becomes much smaller than the SNR of near WDs so that more resources should be allocated to the far WDs. The optimal $\alpha^*$ values obtained by the exact analysis and the approximate analysis agree well overall. However, as $n$ becomes greater than 2.5 and $\lambda$ becomes smaller, the difference between the two $\alpha^*$ values becomes larger because it violates the assumptions of high SNR and sufficient number of accessing WDs.

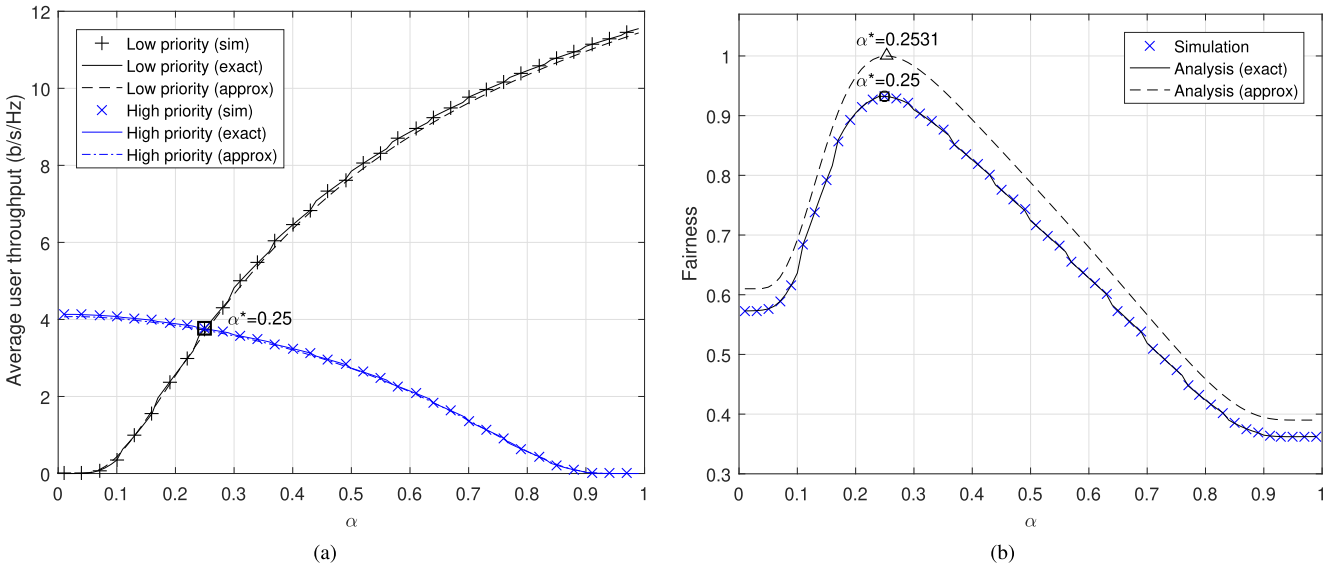


**FIGURE 7.** (a) Average user throughput and (b) fairness vs. allocation ratio $\alpha$ when $\lambda = 1$.

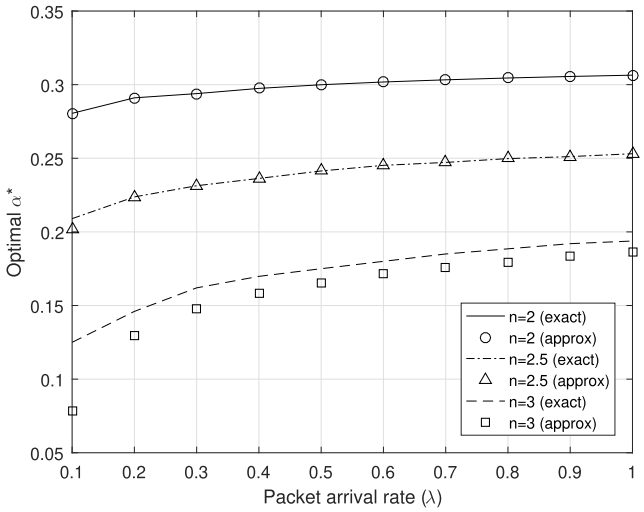


**FIGURE 8.** Optimal allocation ratio ($\alpha^*$) vs. packet arrival rate according to path loss exponent ($n$).

Figure 9 shows the cumulative distribution function of the user throughput when $\lambda = 1$ in terms of all, low-, and high-priority WDs. For the purpose of comparison, we consider the no-priority case and the fixed $\alpha = 0.5$ (i.e., equal resource allocation) case. In the no-priority case, the near WDs labeled ''low'' show a much higher throughput than the far WDs labeled ''high'' as shown in figure 9(b); i.e., the doubly near-far problem is observed. When the optimal $\alpha^*$ is applied, the distribution of the throughput of low-priority WDs and high-priority WDs becomes similar, and thus its throughput distribution of all WDs becomes significantly narrower than that in the no-priority case. This is because the prioritized access control using the optimal $\alpha^*$ gives the far WDs with high priority a longer EH time and more RA slots by sacrificing the near WDs with low priority. Eventually, the doubly near-far problem is alleviated when using the optimal $\alpha^*$. On the other hand, in the fixed $\alpha = 0.5$ case, the throughput distribution of all WDs becomes rather wider than that in the no-priority case as the throughput of the low-priority WDs increases and the throughput of the high-priority WDs decreases inversely. This implies that the wrong choice of $\alpha$ (i.e., simple equal allocation) may have the adverse effect of increasing the throughput difference between near and far WDs.

Figure 10 shows the average user throughput, minimum user throughput, and fairness versus the packet arrival rate. In each scheme of no-priority, fixed $\alpha = 0.5$, and optimal $\alpha^*$, the average user throughputs of all, low-, and high-priority WDs are shown separately. In the no-priority case, the difference in throughput between low- and high-priority WDs is significant so that it shows a low minimum user throughput and a low fairness index. On the other hand, the use of the optimal $\alpha^*$ sacrifices the average user throughput of all WDs, but equalizes the average user throughputs of the low- and the high-priority WDs so that it increases the minimum user throughput and achieves the best fairness index, which eventually contributes to alleviating the doubly near-far problem. However, in the fixed $\alpha = 0.5$ case, the throughput difference between low- and high-priority WDs is greater than that in the no-priority case. Thus, its average user throughput of all WDs increases, but the minimum user throughput deteriorates and the fairness decreases compared with the no-priority case. In terms of throughputs and fairness, there is no difference between the exact $\alpha^*$ and the approximate $\alpha^*$ except when a small number of WDs is accessing with $\lambda = 0.1$. Moreover, the centralized control method of the prioritized access control is plotted as a reference upper bound. This centralized scheme controls that the farthest WD with the minimum rate accesses to the last RA slot to harvest energy for the longest time and the other WDs access the RA slots ahead. Thus, the minimum user rate is maximized and

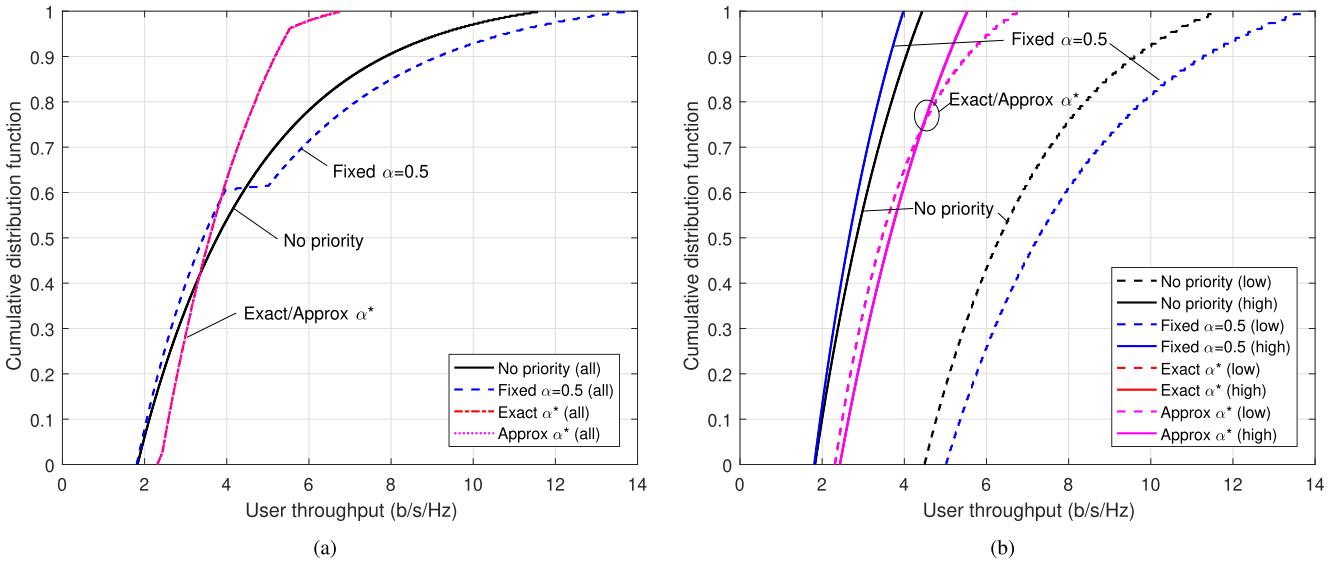


**FIGURE 9.** Cumulative distribution function of user throughput when $\lambda = 1$: (a) all users and (b) low- and high-priority users.

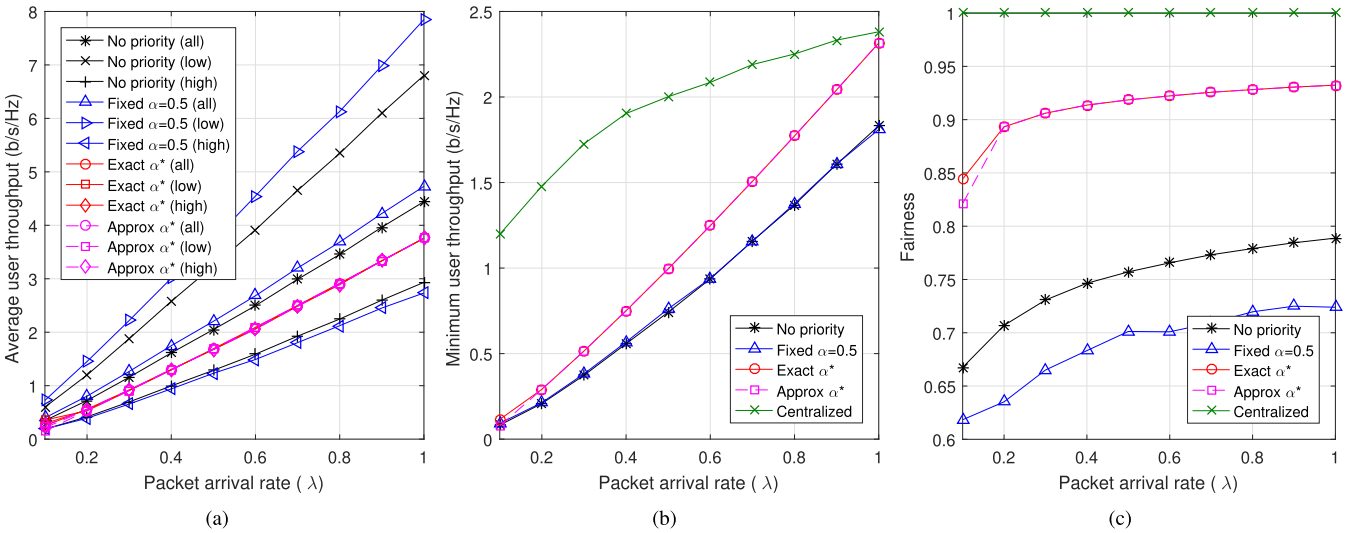


**FIGURE 10.** (a) Average user throughput, (b) minimum user throughput, and (c) fairness vs. packet arrival rate.

the rate of all WDs can be equalize with this minimum user rate, which eventually achieves the maximum fairness index of one, as shown in figure 10(c). It is also shown that the difference between the proposed scheme and the centralized scheme is gradually decreased as $\lambda$ increases.

## VIII. CONCLUSION

In this paper, we designed a slotted ALOHA-based energy-harvesting MAC protocol for WPCNs and maximized its average channel throughput. The analysis results revealed that there always exists a unique optimal number of RA slots greater than the average number of accessing WDs in the high-SNR environment with sufficient accessing WDs, and it depends only on the average $m$SNR of WDs without knowledge of full channel state information. Thereafter, we presented a prioritized access control to alleviate the doubly near-far problem in WPCNs. On the basis of the fact that the proposed protocol has different EH times according to the position of the selected RA slot, we made the near WDs access the former RA slots and the far WDs access the latter RA slots. Similarly, the analysis verified that there exists a unique optimal ratio of RA slots allocated for the low- and high-priority WDs and it depends only on the average $m$SNRs of near and far WDs. The results also showed that the proposed prioritized access control sacrifices the throughput of near WDs, but improves the user fairness and thus mitigates the doubly near-far problem effectively. We expect that in future the proposed protocols will be usefully applied to a distributed WPCN environment that requires low overhead and complexity. For further study, we plan to consider multiple priority levels and optimize the fairness jointly with the throughput.

## APPENDIX
## PROOF OF THE PROPOSITION 1

For $p \geq 1$, the $p$-norm of $\mathbf{z} \in \mathbb{R}^k$ is defined as $||\mathbf{z}||_p = (\sum_{i=1}^{k} |z_i|^p)^{\frac{1}{p}}$. Using this, Jain's fairness index can be rewritten as follows:

$$\mathcal{J}(\mathbf{x}, \mathbf{y}) = \frac{\| \left[\mathbf{x}^T \ \mathbf{y}^T\right] \|_1^2}{(m+n)\| \left[\mathbf{x}^T \mathbf{y}^T\right] \|_2^2}. \tag{35}$$

Note that

$$\begin{aligned}\mathcal{J}(\bar{\mathbf{x}}, \bar{\mathbf{y}}) &= \frac{\| \left[(\frac{1}{m}\mathbf{1}_m\mathbf{1}_m^T\mathbf{x})^T \ (\frac{1}{n}\mathbf{1}_n\mathbf{1}_n^T\mathbf{y})^T\right] \|_1^2}{(m+n)\| \left[(\frac{1}{m}\mathbf{1}_m\mathbf{1}_m^T\mathbf{x})^T \ (\frac{1}{n}\mathbf{1}_n\mathbf{1}_n^T\mathbf{y})^T\right] \|_2^2} \\ &\overset{(a)}{=} \frac{\| \left[\mathbf{x}^T \ \mathbf{y}^T\right] \|_1^2}{(m+n)\| \left[(\frac{1}{m}\mathbf{1}_m\mathbf{1}_m^T\mathbf{x})^T \ (\frac{1}{n}\mathbf{1}_n\mathbf{1}_n^T\mathbf{y})^T\right] \|_2^2}\end{aligned} \tag{36}$$

where (a) comes from $\| \left[(\frac{1}{m}\mathbf{1}_m\mathbf{1}_m^T\mathbf{x})^T \ (\frac{1}{n}\mathbf{1}_n\mathbf{1}_n^T\mathbf{y})^T\right] \|_1 = m(\frac{1}{m}\sum_{i=1}^{m} x_i) + n(\frac{1}{n}\sum_{j=1}^{n} y_j) = \| \left[\mathbf{x}^T \ \mathbf{y}^T\right] \|_1$.

We then have

$$\frac{\mathcal{J}(\mathbf{x}, \mathbf{y})}{\mathcal{J}(\bar{\mathbf{x}}, \bar{\mathbf{y}})} = \frac{\| \left[(\frac{1}{m}\mathbf{1}_m\mathbf{1}_m^T\mathbf{x})^T \ (\frac{1}{n}\mathbf{1}_n\mathbf{1}_n^T\mathbf{y})^T\right] \|_2^2}{\| \left[\mathbf{x}^T \ \mathbf{y}^T\right] \|_2^2} \tag{37}$$

$$\overset{(a)}{=} \left(\frac{\|\mathbf{A}\mathbf{z}\|_2}{\|\mathbf{z}\|_2}\right)^2 \tag{38}$$

$$\overset{(b)}{\leq} \max_i \sigma_{\mathbf{A},i}^2 \tag{39}$$

$$\overset{(c)}{=} 1 \tag{40}$$

where (a) comes from the fact that $\mathbf{z} \triangleq [\mathbf{x}^T \ \mathbf{y}^T]^T$ and

$$\left[(\frac{1}{m}\mathbf{1}_m\mathbf{1}_m^T\mathbf{x})^T \ (\frac{1}{n}\mathbf{1}_n\mathbf{1}_n^T\mathbf{y})^T\right]^T = \left[\begin{array}{c|c} \frac{1}{m}\mathbf{1}_m\mathbf{1}_m^T & \mathbf{0} \\ \hline \mathbf{0} & \frac{1}{n}\mathbf{1}_n\mathbf{1}_n^T \end{array}\right] \times \begin{bmatrix}\mathbf{x} \\ \mathbf{y}\end{bmatrix} = \mathbf{A}\mathbf{z} \tag{41}$$

where $\mathbf{A}$ is a block diagonal matrix, which can be represented in terms of its eigenvalues and eigenvectors as follows:

$$\begin{aligned}\mathbf{A} &= \left[\begin{array}{c|c} \frac{1}{m}\mathbf{1}_m\mathbf{1}_m^T & \mathbf{0}_{m\times n} \\ \hline \mathbf{0}_{n\times m} & \frac{1}{n}\mathbf{1}_n\mathbf{1}_n^T \end{array}\right] \\ &= \left[\begin{array}{c|c} \frac{1}{\sqrt{m}}\mathbf{1}_m & \mathbf{0}_{m\times 1} \\ \hline \mathbf{0}_{n\times 1} & \frac{1}{\sqrt{n}}\mathbf{1}_n \end{array}\right] \times \begin{bmatrix}1 & 0 \\ 0 & 1\end{bmatrix} \times \left[\begin{array}{c|c} \frac{1}{\sqrt{m}}\mathbf{1}_m^T & \mathbf{0}_{1\times n} \\ \hline \mathbf{0}_{1\times m} & \frac{1}{\sqrt{n}}\mathbf{1}_n^T \end{array}\right].\end{aligned} \tag{42}$$

Moreover, Step (b) uses the solution of Rayleigh quotient problems [34], and Step (c) comes from the fact that the largest eigenvalue of $\mathbf{A}$ is 1 from (42). Note that the equality in (b) holds only when $\mathbf{z}^T$ is either $\left[\frac{1}{\sqrt{m}}\mathbf{1}_m^T \ \mathbf{0}_{1\times n}\right]$ or $\left[\mathbf{0}_{1\times m} \ \frac{1}{\sqrt{n}}\mathbf{1}_n^T\right]$. This implies that $\mathcal{J}(\mathbf{x}, \mathbf{y}) < \mathcal{J}(\bar{\mathbf{x}}, \bar{\mathbf{y}})$ for any given $\mathbf{x}$ and $\mathbf{y}$ unless either $\mathbf{x}$ or $\mathbf{y}$ has all components equal to zero.

## REFERENCES

[1] S. Bi, Y. Zeng, and R. Zhang, "Wireless powered communication networks: An overview," *IEEE Wireless Commun.*, vol. 23, no. 2, pp. 10–18, Apr. 2016.
[2] S. Bi, C. K. Ho, and R. Zhang, "Wireless powered communication: Opportunities and challenges," *IEEE Commun. Mag.*, vol. 53, no. 4, pp. 117–125, Apr. 2015.
[3] H. Ju and R. Zhang, "Throughput maximization in wireless powered communication networks," *IEEE Trans. Wireless Commun.*, vol. 13, no. 1, pp. 418–428, Jan. 2014.
[4] D. Niyato, P. Wang, and D. I. Kim, "Performance analysis and optimization of TDMA network with wireless energy transfer," *IEEE Trans. Wireless Commun.*, vol. 13, no. 8, pp. 4205–4219, Aug. 2014.
[5] L. Liu, R. Zhang, and K.-C. Chua, "Multi-antenna wireless powered communication with energy beamforming," *IEEE Trans. Commun.*, vol. 62, no. 12, pp. 4349–4361, Dec. 2014.
[6] H. Ju and R. Zhang, "Optimal resource allocation in full-duplex wireless-powered communication network," *IEEE Trans. Commun.*, vol. 62, no. 10, pp. 3528–3540, Oct. 2014.
[7] X. Kang, C. K. Ho, and S. Sun, "Full-duplex wireless-powered communication network with energy causality," *IEEE Trans. Wireless Commun.*, vol. 14, no. 10, pp. 5539–5551, Oct. 2015.
[8] W. Shin, M. Vaezi, J. Lee, and H. V. Poor, "Cooperative wireless powered communication networks with interference harvesting," *IEEE Trans. Veh. Technol.*, vol. 67, no. 4, pp. 3701–3705, Apr. 2018.
[9] Powercast Corp. *RF Energy Harveseting & Wireless Power*. Accessed: Sep. 24, 2018. [Online]. Available: http://www.powercastco.com
[10] V. Namboodiri, M. Desilva, K. Deegala, and S. Ramamoorthy, "An extensive study of slotted ALOHA-based RFID anti-collision protocols," *Comput. Commun.*, vol. 35, no. 16, pp. 1955–1966, Sep. 2012.
[11] J. Kim and J.-W. Lee, "Performance analysis of the energy adaptive MAC protocol for wireless sensor networks with RF energy transfer," in *Proc. Int. Conf. ICT Converg. (ICTC)*, Sep. 2011, pp. 14–19.
[12] M. Y. Naderi, P. Nintanavongsa, and K. R. Chowdhury, "RF-MAC: A medium access control protocol for re-chargeable sensor networks powered by wireless energy harvesting," *IEEE Trans. Wireless Commun.*, vol. 13, no. 7, pp. 3926–3937, Jul. 2014.
[13] P. Tamilarasi and B. Lavenya, "Energy and throughput enhancement in wireless powered communication networks using RF-MAC and CSMA," in *Proc. Int. Conf. Innov. Inf., Embedded Commun. Syst. (ICIIECS)*, Mar. 2015, pp. 1–4.
[14] S. Bi, Y. J. Zhang, and R. Zhang, "Distributed scheduling in wireless powered communication network: Protocol design and performance analysis," in *Proc. Int. Symp. Modeling Optim. Mobile, Ad Hoc, Wireless Netw. (WiOpt)*, May 2017, pp. 1–7.
[15] T. Ha, J. Kim, and J.-M. Chung, "HE-MAC: Harvest-then-transmit based modified EDCF MAC protocol for wireless powered sensor networks," *IEEE Trans. Wireless Commun.*, vol. 17, no. 1, pp. 3–16, Jan. 2018.
[16] H.-H. Choi, J.-M. Moon, I.-H. Lee, and H. Lee, "Carrier sense multiple access with collision resolution," *IEEE Commun. Lett.*, vol. 17, no. 6, pp. 1284–1287, Jun. 2013.
[17] M. Moradian and F. Ashtiani, "Throughput analysis of a slotted ALOHA-based network with energy harvesting nodes," in *Proc. IEEE Int. Symp. Pers. Indoor Mobile Radio Commun. (PIMRC)*, Sep. 2012, pp. 351–356.
[18] O. Briante, A. M. Mandalari, A. Molinaro, G. Ruggeri, F. Vazquez-Gallego, and J. Alonso-Zarate, "Duty-cycle optimization for machine-to-machine area networks based on frame slotted-ALOHA with energy harvesting capabilities," in *Proc. 20th Eur. Wireless Conf.*, May 2014, pp. 1–6.
[19] F. Iannello, O. Simeone, and U. Spagnolini, "Dynamic framed-ALOHA for energy-constrained wireless sensor networks with energy harvesting," in *Proc. IEEE Global Telecommun. Conf. (GLOBECOM)*, Dec. 2010, pp. 1–6.
[20] S. Wu, Y. Chen, K. K. Chai, F. Vazquez-Gallego, and J. Alonso-Zarate, "Analysis and performance evaluation of dynamic frame slotted-ALOHA in wireless machine-to-machine networks with energy harvesting," in *Proc. IEEE Globecom Workshops*, Dec. 2014, pp. 1081–1086.
[21] M. Kaus, J. Kowal, and D. U. Sauer, "Modelling the effects of charge redistribution during self-discharge of supercapacitors," *Electrochim. Acta*, vol. 55, no. 25, pp. 7516–7523, 2010.
[22] H. Lee, K.-J. Lee, H. Kim, B. Clerckx, and I. Lee, "Resource allocation techniques for wireless powered communication networks with energy storage constraint," *IEEE Trans. Wireless Commun.*, vol. 15, no. 4, pp. 2619–2628, Apr. 2016.

[23] C. Xu, M. Zheng, W. Liang, H. Yu, and Y.-C. Liang, "End-to-end throughput maximization for underlay multi-hop cognitive radio networks with RF energy harvesting," *IEEE Trans. Wireless Commun.*, vol. 16, no. 6, pp. 3561–3572, Jun. 2017.
[24] C. Xu, W. Liang, and H. Yu, "Green-energy-powered cognitive radio networks: Joint time and power allocation," *ACM Trans. Embedded Comput. Syst.*, vol. 17, no. 1, Nov. 2017, Art. no. 13.
[25] O. Ozel, K. Tutuncuoglu, J. Yang, S. Ulukus, and A. Yener, "Transmission with energy harvesting nodes in fading wireless channels: Optimal policies," *IEEE J. Sel. Areas Commun.*, vol. 29, no. 8, pp. 1732–1743, Sep. 2011.
[26] C. K. Ho and R. Zhang, "Optimal energy allocation for wireless communications with energy harvesting constraints," *IEEE Trans. Signal Process.*, vol. 60, no. 9, pp. 4808–4818, Sep. 2012.
[27] X. Kang, Y.-K. Chia, C. K. Ho, and S. Sun, "Cost minimization for fading channels with energy harvesting and conventional energy," *IEEE Trans. Wireless Commun.*, vol. 13, no. 8, pp. 4586–4598, Aug. 2014.
[28] X. Lu, P. Wang, D. Niyato, D. I. Kim, and Z. Han, "Wireless networks with RF energy harvesting: A contemporary survey," *IEEE Commun. Surveys Tuts.*, vol. 17, no. 2, pp. 757–789, 2nd Quart., 2015.
[29] X. Hou and H. Kayama, "Demodulation reference signal design and channel estimation for LTE-Advanced uplink," in *Advances in Vehicular Networking Technologies*. Rijeka, Croatia: InTech, 2011, pp. 417–432.
[30] A. Papoulis and S. Pillai, *Probability—Random Variables and Stochastic Processes*. New York, NY, USA: McGraw-Hill, 2002.
[31] L. Song and D. Hatzinakos, "Dense wireless sensor networks with mobile sinks," in *Proc. IEEE Int. Conf. Acoust., Speech, Signal Process. (ICASSP)*, vol. 3, Mar. 2005, pp. 677–680.
[32] R. K. Jain, D.-M. W. Chiu, and W. R. Hawe, "A quantitative measure of fairness and discrimination for resource allocation in shared computer systems," Eastern Res. Lab., Digit. Equip. Corp., Hudson, MA, USA, Tech. Rep. DEC-TR-301, 1984, vol. 38.
[33] F. Topse, "Some bounds for the logarithmic function," *RGMIA Res. Rep. Collection*, vol. 7, no. 2, 2004, Art. no. 6.
[34] R. A. Horn and C. A. Johnson, *Matrix Analysis*. Cambridge, U.K.: Cambridge Univ. Press, 1985, pp. 176–180.

**HYUN-HO CHOI** (S'02–M'07) received the B.S., M.S., and Ph.D. degrees from the Department of Electrical Engineering, Korea Advanced Institute of Science and Technology, South Korea, in 2001, 2003, and 2007, respectively. From 2007 to 2011, he was a Senior Engineer at the Communication Lab, Samsung Advanced Institute of Technology, South Korea. Since 2011, he has been a Professor with the Department of Electrical, Electronic, and Control Engineering, and the Institute for Information Technology Convergence, Hankyong National University, South Korea. His current research interests include bio-inspired algorithms, distributed optimization, machine learning, wireless energy harvesting, mobile ad hoc networks, and next-generation wireless communication. He is a member of IEICE, KICS, and KIICE. He was a co-recipient of the SAIT Patent Award in 2010, the Paper Award at the Samsung Conference in 2010, the Excellent Paper Award at ICUFN 2012, the Best Paper Award at ICN 2014, and the Best Paper Award at Qshine 2016.

**Wonjae Shin** (S'14–M'17) received the B.S. (Hons.) and M.S. degrees from the Korea Advanced Institute of Science and Technology in 2005 and 2007, respectively, and the Ph.D. degree from the Department of Electrical and Computer Engineering, Seoul National University (SNU), South Korea, in 2017. From 2007 to 2014, he was a Member of Technical Staff with the Samsung Advanced Institute of Technology and Samsung Electronics Company Ltd., South Korea, where he contributed to next generation wireless communication networks, especially for 3GPP LTE/LTE-advanced standardizations. He was a Visiting Scholar and a Post-Doctoral Research Fellow at Princeton University, Princeton, NJ, USA, from 2016 to 2018. He is currently an Assistant Professor with the Department of Electronics Engineering, Pusan National University, Busan, South Korea. His research interests are in the design and analysis of the future wireless communications, such as interference-limited networks. He received the Best Ph.D. Dissertation Award from SNU in 2017, the Gold Prize from the IEEE Student Paper Contest (Seoul Section) 2014, and the Award of the Ministry of Science and ICT of Korea in IDIS-Electronic News ICT Paper Contest 2017. He was a co-recipient of the SAIT Patent Award in 2010, the Samsung Journal of Innovative Technology in 2010, the Samsung HumanTech Paper Contest in 2010, and the Samsung CEO Award in 2013. He was a recipient of several fellowships, including the Samsung Fellowship Program in 2014 and the SNU Long Term Overseas Study Scholarship in 2016. He was recognized as an Exemplary Reviewer of the IEEE Wireless Communications Letters in 2014.